RICHARD J. NEVES

Geist Shell 2005

ELSEVIER

Geochimica et Cosmochimica Acta, Vol. 69, No. 14, pp. 3545–3554, 2005
Copyright © 2005 Elsevier Ltd
Printed in the USA. All rights reserved
0016-7037/05 $30.00 + .00

doi:10.1016/j.gca.2005.03.010

Stable carbon isotopes in freshwater mussel shells: Environmental record or marker for metabolic activity?

JUERGEN GEIST,[1,*] KARL AUERSWALD,[2] and ARNOUD BOOM[†,2]

[1]Wildlife Biology and Wildlife Management Unit, TU Muenchen, Wissenschaftszentrum Weihenstephan, D-85350 Freising, Germany
[2]Grassland Science, TU Muenchen, Wissenschaftszentrum Weihenstephan, D-85350 Freising, Germany

(*Received November* 12, 2004; *accepted in revised form March* 7, 2005)

Abstract—Mussel shells have been used in a number of paleoecological and environmental studies. The interpretation of stable carbon isotopic composition of shell material is still controversial. The carbon for shell carbonate precipitation can either be derived from ambient dissolved inorganic carbon (DIC), with shells recording environmental signals, or from metabolic CO_2, with the potential to disguise environmental signals. To gain insight into this question, we investigated four nearly 100-yr long-term records of aragonite shells from an extant freshwater bivalve species, the endangered freshwater pearl mussel (*Margaritifera margaritifera* L.). Single growth increments of the outer prismatic and the inner nacreous zones were successfully and easily separated with a simple heat treatment for chronological analyses of $\delta^{13}C$ in single layers of each zone. Autocorrelation and semivariance statistical methods reveal that mussels show distinct individual signal patterns, which extend up to 25 yr. Signal patterns are reliably reproduced with replicate samples from defined layers within one shell and show similar patterns with a slight offset for inner nacreous and outer prismatic layers for individual animals. Mussels exposed to the same environmental conditions exhibit distinct and contradictory signature patterns, which do not match between individuals. This observation can only be explained by strong metabolic influences on shell precipitation. Environmental changes in pH, temperature, electric conductivity and atmospheric carbon signature had no or little (<5%) influence, whereas body tissue protein and body tissue $\delta^{13}C$ signatures negatively correlated with the youngest produced shell $\delta^{13}C$ signatures, indicating that respiration causes a preferential loss of light isotopes from body mass and an inverse enrichment in shell aragonite. Hence, the shells of the freshwater pearl mussel yield a long-term record of metabolic activity, whereas the use of $\delta^{13}C$ in these shells as recorder for environmental signals is questionable. This may also be true for shells from other species, for which metabolic carbon incorporation has been acknowledged. *Copyright © 2005 Elsevier Ltd*

1. INTRODUCTION

Mussel shells have been used in a number of paleoecological and environmental studies. While stable oxygen isotopic signatures in mussel shells have proved to be reliable recorders of environmental parameters (e.g., Epstein et al., 1953; Tripati et al., 2001), the interpretation of stable carbon isotopic composition of shell material remains contentious. Some isotopic studies on shells have shown that the stable isotopic composition ($\delta^{13}C$) of the shell carbonate is governed by the $\delta^{13}C$ of dissolved inorganic carbon (DIC) and therefore records changes in environmental variables such as pH, temperature, and salinity (e.g., Craig, 1953; Keith et al., 1964; Mook, 1971; Fritz and Poplawski, 1974; Donner and Nord, 1986). Under ideal conditions, shell carbonate would be precipitated in equilibrium, resulting in calcite which is +1‰ enriched in comparison with bicarbonate, and aragonite that is +2.7‰ enriched (Romanek et al., 1992). On the other hand, shell carbonates were often found not to reflect the predicted equilibrium fractionation, being in general less enriched than predicted in ^{13}C (e.g., Klein et al., 1996; McConnaughey et al., 1997; McConnaughey, 2003; Kaandorp et al., 2003). Most authors explain this offset by a contribution of metabolic carbon (Tanaka et al., 1986; Klein et al., 1996; Veinott and Cornett, 1998; Vander Putten et al., 2000). Thus, researchers have indirectly acknowledged an influence of the food source, which is reflected in a certain percentage of metabolic derived carbon within the carbonate. Despite this, it is often stated that the total contribution of metabolic CO_2 in aquatic invertebrates is generally low to insignificant, suggesting that kinetic effects can explain nonequilibrium fractionations (McConnaughey et al., 1997; McConnaughey, 2003). In contrast, Dettman et al. (1999) found $\delta^{13}C$ values of aragonite-forming freshwater bivalves with a highly variable offset to equilibrium values, suggesting a significant and variable incorporation of metabolic carbon into shell carbonate. Despite the observed isotopic disequilibrium of carbonate formation, shell records are frequently compared to or assumed to reflect changes in ambient $\delta^{13}C_{DIC}$.

The freshwater pearl mussel (*Margaritifera margaritifera* L.) is a long-lived species which is sessile or relative immobile during its adult phase. It produces a shell of well-defined material with annual increments. This combination offers a great potential for chronological analyses of shell $\delta^{13}C$ signatures to reveal changes within its environment. Freshwater pearl mussels are widely distributed in the holarctic range. They attain individual ages of more than 100 yr (Bauer, 1992). The species is nowadays critically endangered and analyses of biochronological records in shell material may help to find reasons for the species' low and decreasing vitality during the last decades. Like other mussels from cold and temperate

* Author to whom correspondence should be addressed (geist@wzw.tum.de).
† *Present address:* Department of Geography, University of Leicester, United Kingdom.

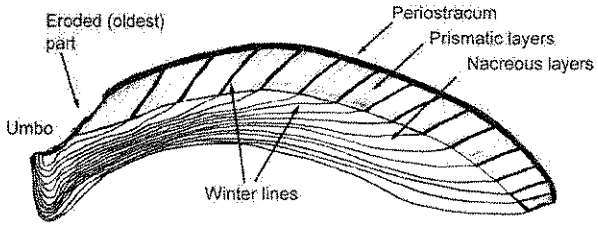

Fig. 1. Schematic of the cross section of a *Margaritifera margaritifera* shell.

climates, *M. margaritifera* shells have annual growth increments (Fig. 1), analogous to tree rings, with shell formation during summer and a reduced or ceased carbonate deposition at low temperatures during winter (e.g., Siegele et al., 2001). The inorganic carbon in *M. margaritifera* shells is carbonate in the form of aragonite (Carell et al., 1987; Nyström et al., 1995). Visible opaque, organic scleroprotein-rich ridges are produced during winter and separate the aragonite increments of maximum growth from summer seasons. These layers allow analyses of time scale series of samples. Once deposited, the carbonate is immobilized and resistant to subsequent changes (Lindh et al., 1988). *M. margaritifera* mussel shell records have been studied to reveal changes in elemental composition of the shell material and have been used as environmental indicators for eutrophication and acidification (e.g., Carell et al., 1987; Lindh et al., 1988; Mutvei and Westermark, 2001 and references therein).

An evaluation of the influences on shell isotopic chemistry is important for the interpretation of such values in the context of environmental or paleoenvironmental studies. We present a novel and simple method to sample annual growth layers from the outer prismatic and the inner nacreous zone of mussel shells, by removing the organic carbon, and we test the hypothesis that shell $\delta^{13}C$ signature is controlled by environmental variables. If this is the case, different individuals exposed to the same environment should exhibit similar $\delta^{13}C$ values and their signature should synchronously change with changing environment. Hence, we use old animals from one species and from the same location. Over their life span of 100 yr, changes in environmental conditions can be chronicled.

2. MATERIALS AND METHODS

2.1. Sampling Site

Freshwater pearl mussels typically inhabit clear streams which are low in lime and nutrients. Four specimens originating from the same population were collected in August 2001 from a small headwater stream from the Elbe drainage system in the Fichtel Mountains close to the border between Germany and the Czech Republic. Specimens were labeled Z1, Z2, Z3 and Z12. All individuals were found in close vicinity, belonged to one large mussel bank covering an area of 5 m by 1 m and were exposed to identical environmental conditions. Daily observation of the stream and its strictly protected mussel population enabled us to sample four pearl mussels shortly after they had died. The mussels had shell lengths of 10.8 cm (Z1), 9.5 cm (Z2), 9.2 cm (Z3) and 11.0 cm (Z12). Exact sampling location will be provided on demand but is not published here, as illegal pearl fishing is still a threat to the endangered and protected species.

At the sampling site, the stream is on average 1.5 m wide and 25 cm deep. The stream is oligotrophic and the turbulent current results in a well-mixed water body. Oxygen concentrations and saturations measured in the field in 14-d intervals over 3 yr showed an arithmetic mean of 11.1 mg/L (standard deviation, SD = 1.4), equivalent to average saturation levels of 90% (SD = 2.3). Biologic oxygen demand over 5 d (BOD_5) was permanently low, with an average of only 1.1 mg/L (SD = 0.5). Calcium concentrations averaged 7.0 mg/L with a standard deviation of 1.7 over the year. Data on pH, electrical conductivity and water temperature were available from 1987 to 2003 (provided by the Water Authority at Hof). Every year instantaneous measurements were taken during 1 d before the onset of the growing period (mostly in February), 1 d during the early growing period (mostly in April), 1 d in the middle of the growing period (mostly in August) and 1 d at the end of the growing period (mostly in October). Additionally, 5-d averages of air temperature measured at a meteorological station 30 km away from the brook were used to extend the temperature data set back to 1947 (source: German Meteorological Service) as air and water temperature were closely linearly related ($r^2 = 0.93$ for $n = 67$). The water temperature ranged between 0 and 15°C and had a seasonal trend from ~2°C in January, a rise to 15°C in July and a decrease to 4°C in November. The pH mostly varied between 6 and 7, with snowmelt runoff early in the year causing the lowest pH of around 6.3. The average pH increased until the end of the year to 7.0. Low pH values (down to 5.5) caused by interflow runoff during heavy rainstorms are also possible throughout the year (Auerswald, 1990). No long-term trends in pH or temperature extending over several years were obvious from the data (Fig. 2). Conductivity varied between 70 and 140 μs/cm, mostly with higher values during summer and lower values during winter and spring season, when water flow increases. Average values of temperature, pH and conductivity were calculated for the growth periods and compared with annual isotopic signatures, respectively.

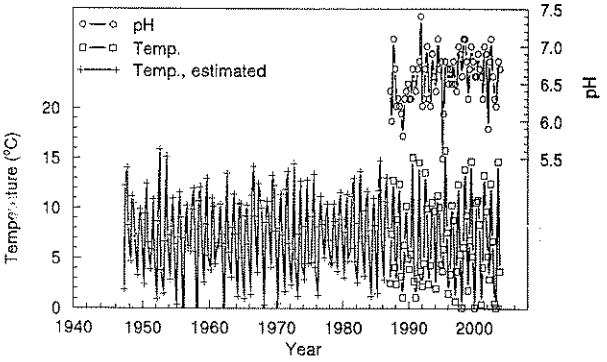

Fig. 2. Instantaneous measurements of pH and temperature from the brook water between 1987 and 2003. Water temperature was extended to 1947 by using daily averages of air temperature and a regression between air and water temperature.

2.2. Shell Preparation

Margaritifera shells are composed of three principal zones: a moderately thick, organic periostracum on the outside of the shell preventing dissolution, followed by two aragonite containing zones, the outer prismatic and the inner nacreous layers (Fig. 1). The oldest part of the shell is the umbo, where erosion of periostracum and aragonite occurs in older individuals.

Sampled mussels were preserved by freezing at −20°C. Soft tissue was manually removed and the shells cleaned and rinsed with H_2O (deionized) both inside and outside. For analyses of $\delta^{13}C$ of shell material, valves were separated by hand and from each shell, a 10 mm wide section was cut with a saw from the umbo region to the posterior-ventral edge, representing the axis of maximum growth and thus yielding the most detailed archival information (Siegele et al., 2001). After drying at 50°C for 12 h, shell sections were weighed and heated at 550°C for 2 h in a muffle oven for complete combustion of organic components. After cooling down, the loss of weight on ignition was determined. The loss of organic material concentrated at the winter lines and allowed an easy separation of growth increments in both the

outer prismatic zone and the inner nacreous zone, whereas the protein-rich periostracum simply fell apart and its remains were removed with a brush before sampling. The roofing-tile like layers of the outer prismatic zone were chronologically sampled with a scalpel blade starting close to the eroded part of the shell near the umbo towards the youngest layer at the ventral edge, which was produced in the final year of growth. The sampling of the inner nacreous layers was started from the inside of the shell towards the outside, representing a chronological order from the final year of growth towards older layers. Growth layers in both zones, outer prismatic and inner nacreous usually correspond with years. However, growth interruptions during summer may result in overestimation of years and thin organic layers corresponding with short and warm winters can be overseen and thus two layers sampled as one. Both situations are rare and partly compensate each other in the long-term trend. Although visual inspection allowed an easy identification of single layers, it was occasionally not possible to separate them due to the high age (>80 yr) and slow growth of pearl mussels at the sampling site (maximum shell thickness before ignition: 3 mm; average layer thickness often around 0.7 mm for prismatic layers with a decreasing tendency towards ventral edges and more than ten times smaller for nacreous layers). In such cases, coherent layers were sampled together and the value was assigned to both layers. For one shell (Z3) inner nacreous and outer prismatic layers were sampled from both valves independently to test the reliability of the method.

2.3. Stable Carbon Isotope Analysis

Growth layers were ground to a fine powder with a carbon-free agate mortar and pestle. Three mg subsamples (±0.1 mg) were then enclosed in tin cups (4 × 6 mm) and combusted in an elemental analyzer (Carlo Erba NA 1108, Milan), interfaced (ConFlo II, Finnigan MAT, Bremen) to an isotope ratio mass spectrometer (Delta Plus, Finnigan MAT, Bremen). Different tissues of the soft parts of the mussels (mantle margin, mantle interior, mantle total, adductor muscle, gills, foot and digestive gland/visceral mass) and samples of potential food sources (alder leaves, roots from ambient riparian vegetation, coarse detritus, fine detritus and fine suspended particulates >30 μm) were freeze-dried, ground and ball milled before analyses. Organic shell material was analyzed after ball-milling shell material and subsequent HCl fumigation of the moistened sample material, previously weighed into Ag cups (Harris et al., 2001). Nitrogen signatures were directly measured from ball-milled untreated samples. Proteins and lipids were separately extracted from the body soft tissue of the four specimens and analyzed for $\delta^{13}C$ and $\delta^{15}N$, according to Rossmann (2001) and Piasentier et al. (2003).

The data are presented as $\delta^{13}C$ (‰) relative to PDB standard. For possible food sources and tissue material $\delta^{15}N$ (‰) was additionally measured in relation to nitrogen in air. $\delta^{13}C$ and $\delta^{15}N$ were calculated as follows: $\delta X = [(R_{sample}/R_{standard}) - 1] \times 10^3$, where δX is $\delta^{13}C$ or $\delta^{15}N$, and R is the respective $^{13}C/^{12}C$ or $^{15}N/^{14}N$ ratio. The working gas standards for C and N isotope determination were calibrated against the laboratory standard, a fine ground wheat flour of known C and N isotope composition ($\delta^{13}C$ −26.54‰ and $\delta^{15}N$ +2.61‰), which had previously been calibrated against IAEA-CH6 and IAEA-NO3 secondary isotope standards. The same working standard was run regularly after every 10th sample as a control. Blank determinations were done routinely before each batch of samples (including working standards) by running empty tin cups. The $\delta^{15}N$ data were blank-corrected. The external precision (standard deviation, SD) was ±0.2‰ for $\delta^{13}C$ and ±0.3‰ for $\delta^{15}N$.

A series of additional tests were carried out to verify the impact of the shell analyses procedures in comparison with conventional methods. X-ray diffraction analysis was used to investigate conversion of aragonite to calcite. Removal effectiveness of organic components during heating was verified by two independent experiments: firstly, removal of N in the shell samples was measured by combustion with the elemental analyzer. Additionally, carbon removal efficiency was investigated at various temperatures, using a mixture of silicate powder and wheat flour. Accuracy of the measurements in comparison with standard phosphoric acid digestion technique using Kiel device was tested by splitting samples and analyzing $\delta^{13}C$ signatures of powdered shell material (each 15 samples before and after ignition at 550°C) in two laboratories.

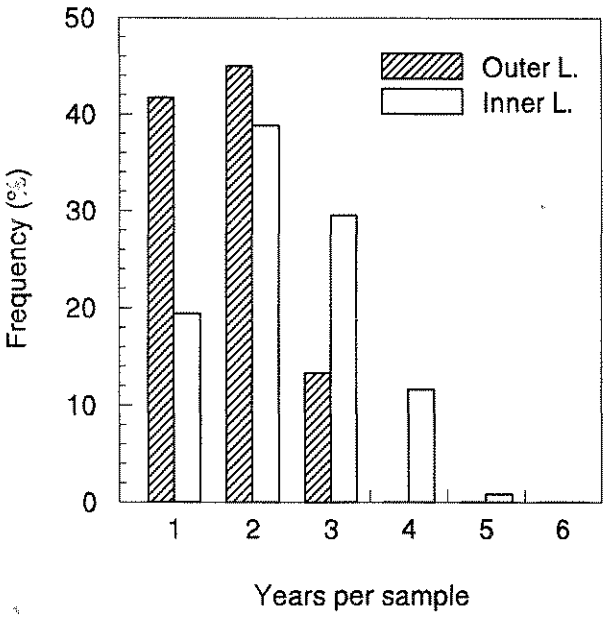

Fig. 3. Number of years per sample of the outer and inner layers as estimated from visual inspection.

2.4. Statistical Analysis

Autocorrelation analysis and geostatistical analysis (semivariograms) were applied to detect and determine the extent of layer overlapping signal trends in $\delta^{13}C$. Experimental semivariograms for $\delta^{13}C$ were computed to determine the extent and range of autocorrelation by pooling the inner and outer layers of all shells. Semivariograms quantify the average dissimilarity (= semivariance) of a property (e.g., the signature) depending on the distance (= lag), which is in this case the number of layers between two samples. Spherical models were fitted to the experimental semivariograms. The intercept on the y-axis (semivariance for zero lag) is called the nugget effect and quantifies local variability or "noise" within the data. With increasing lag, semivariance approaches a plateau, which is called the sill. The sill of the semivariogram quantifies the variation in signature over distances beyond the range of the autocorrelation. A large difference between sill and nugget effect indicates a pronounced pattern, while no pattern exists where the sill equals the nugget effect. The range corresponds to the lag beyond which the sill is reached. It quantifies the maximum distance over which pairs of observations remain correlated. For theory and details of geostatistical analysis, see Nielsen and Wendroth (2003). Most statistical calculations were done with SAS (version 8; SAS Institute, Cary, NC, USA).

3. RESULTS AND DISCUSSION

3.1. Sampling Method and Reliability

Heating at 550°C indicated 7%–8% (wt.) organic material (av. = 7.6%, SD = 0.7%) and was an easy and effective method to remove the periostracum, separate the outer prismatic and inner nacreous layers and sample distinct growth increments within these zones. More than 60 layers per shell could be separated. This method allowed an easy sampling of the roofing-tile-like prismatic (= outer) layers. Single "roofing tiles" from the outer prismatic zone consisted of one or two growth increments in 90% of all cases, whereas separation was less effective for the thinner inner nacreous layers where the samples mostly consisted of two growth increments (Fig. 3).

For the two replicates of mussel Z3, similar numbers of years were sampled (83 vs. 86 yr in outer layers and 49 vs. 47 yr in inner layers).

While the outer layers are preferable to study interannual variations, it has to be considered that erosion occurs at the umbo region of old shells in freshwater pearl mussels and some other mussel species. This will reduce the time span of the archive. Nevertheless, for mussel Z3 more outer layers than inner layers were found, which may depend on the specific erosion pattern in this particular shell.

Other sampling techniques for shell material, such as micro drilling and milling of shell material at depth intervals of 15–30 μm (Dettman and Lohmann, 1993; Dettman et al., 1999; Wurster et al., 1999), are able to deliver a higher time resolution than the method described in this paper and even allow studies on intra-annual variation. Such techniques, however, require specific equipment and sampling may be restricted to certain areas of the shell because of geometry requirements of the sampling technique (Dettman et al., 1999). Furthermore, drilling techniques likely increase the danger of yielding mixtures of nacreous and prismatic layers or different annual layers within these zones, which may especially arise when mussels with thin shells, high individual age and moderate growth rates are selected for investigation. For studies on long-term trends and comparisons of average values between growth increments (usually corresponding with years in cold and temperate climate zones), the methodology suggested in this paper allows an easy and reliable sampling of defined layers for both, the prismatic and inner nacreous zone, separately. However, each sampling technique is based on the assumption that an annual growth pattern in the shell with organic-rich layers and ceasing carbonate precipitation at lower temperatures during winter prevails, and is susceptible to counting errors. For *M. margaritifera* these errors are considered to be small, and the tree ring analogous shell growth patterns are regularly used by field biologists for individual age determination in the species. The difference of growth layers sampled in both valves of Z3 was 3% for the outer prismatic and 4% for the inner nacreous layers, respectively, which is in good agreement with an estimated counting error of ±5% in 100 yr for *M. margaritifera* reported by Carell et al. (1987). As freshwater pearl mussels used in this study were comparatively old and as the species is reported to grow in approximately asymptotic fashion (Hastie et al., 2000), the use of younger and faster growing individuals from this species or the use of generally faster growing mussel species will probably allow further reduction of this error. For analyses of time trends, small errors in layer sampling will be of minor importance. In cases where more exact layer sampling is required, the analyses of several independently sampled stripes from both valves of one shell and subsequent comparisons of time trends will improve dating.

A series of additional tests (XRD-analysis, comparison of the method with standard phosphoric acid digestion technique, C and N measurements for testing complete combustion of organic matter in the shell material during heating) proved the reliability of the methods described in this paper. Aragonite was completely converted to calcite but the procedure proved not to systematically change the $\delta^{13}C$ signatures (average difference between heated and untreated samples determined by standard phosphoric acid digestion: $-0.2‰^{n.s.}$). The only effect of the heating was an increase in scatter. Therefore, the identified patterns in subsequent layers may in fact be even more pronounced. The ignition process at 550°C removes all the organic carbon and 97% of the nitrogen and was found to be less effective at lower temperatures. Assuming a worst case situation, the complete conversion of all potentially remaining organic carbon to carbonate during the heating (assuming a $\delta^{13}C$ signature of $-27‰$), the $\delta^{13}C$ signature of shell samples could only be shifted by a maximum of 0.5‰. Even these worst case assumptions would thus neither change the ranking of samples nor limit the comparability of patterns.

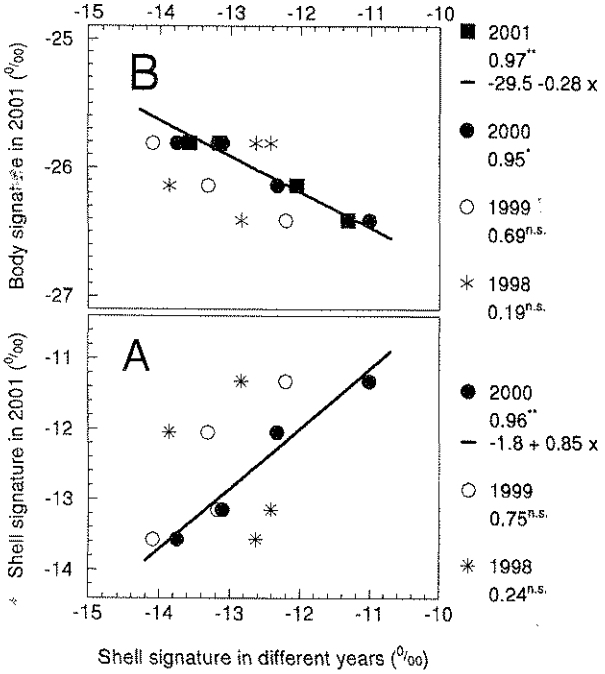

Fig. 4. Correlation of the $\delta^{13}C$ signature of shell carbonate from the last (1998–2000) outer layers with the youngest (2001) shell carbonate (A) and with organic carbon in body tissue (B).

3.2. Mussels Display Long-Term $\delta^{13}C$ Patterns

Values for $\delta^{13}C$ in *M. margaritifera* shells ranged from $-10‰$ to $-15‰$. Similar values were described for *Elliptio complanata*, another freshwater mussel species, where maximum range of $\delta^{13}C$ variation was $-9.0‰$ to $-14.5‰$ and annual variations of maximum 2‰ (Veinott & Cornett, 1998). In generally faster growing zebra mussels, Fry et al. (2003) found less negative carbon isotopic signatures, varying between $-8‰$ to $-11‰$ in one river but to be quite constant around $-9‰$ at one location, with slight seasonal variation of less than 0.5‰.

Autocorrelation analyses showed that $\delta^{13}C$ signatures were similar in adjacent growth layers, but dissimilarity increases with distance. Signatures of the youngest layer (2001) from different mussels closely correlated ($r^2 = 0.96$ with $n = 5$, outer prismatic layers) with the previous layers of the same mussel (Fig. 4A). With increasing distance to the latest produced layer, correlation decreased sharply. This indicated that

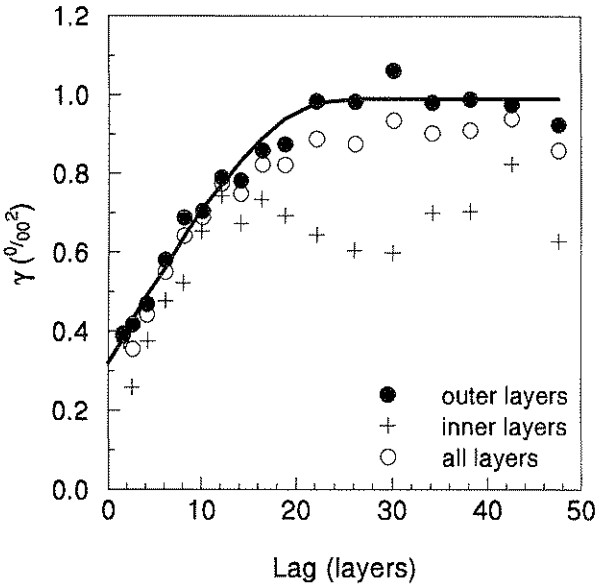

Fig. 5. Pooled semivariograms of $\delta^{13}C$ signature for inner, outer, and all layers; parameters of the spherical model calculated for outer layers (line) are provided in Table 1.

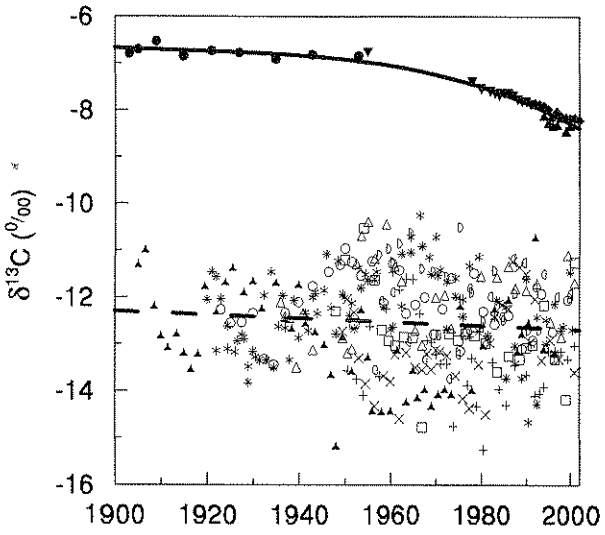

Fig. 6. Comparison of shell signature (crosses for outer layers; open symbols for inner layers) with atmospheric CO_2 signature (solid symbols) reconstructed from annual averages from the Siple ice core (Antarctica; Friedli et al., 1986), and the atmospheric measuring stations of Mauna Loa (Hawaii, Keeling et al., 1995), Hungary, Ulan Uul (Mongolia) and Ochsenkopf (Germany) (http://www.cmdl.noaa.gov/ccgg/iadv/); regression lines: air with $r^2 = 0.9787$ for $n = 42$, shells with $r^2 = 0.0083$ for $n = 345$.

(i) mussels show distinct individual signatures differing by 3‰, although they grew in close vicinity, and (ii) that these patterns cover several years.

Geostatistical analysis allowed a more rigid assessment of this phenomenon by taking all layers of all mussels simultaneously into account. This also showed that adjacent layers were autocorrelated and did not show independent signals. The range shows that the autocorrelation extended up to 25 layers (Fig. 5, Table 1). The resulting temporal pattern (sill) contributed ~70% to the total variation (sill + nugget), while the nugget effect, which quantifies the variability within a certain layer, contributed the remaining 30%. Hence, 70% of the signal can be interpreted as a nonrandom time trend and 30% of the signal is a layer-individual (= annual) signal plus the analytical error.

The nugget effect, sill and range were smaller for the inner nacreous layers than for the outer prismatic layers. All three effects resulted from the higher proportion of composite samples of the thin nacreous layers.

3.3. Carbon Sources for Aragonite Formation

Industrialization linked with burning of fossil fuels has changed atmospheric CO_2 signature during the last decades towards more negative $\delta^{13}C$ values. This atmospheric trend should have caused an analogous increase in the part of the DIC, which may be directly derived from the atmospheric pool and in the signature of new primary biomass, which is a potential food source for freshwater pearl mussels. Chronological samples of shell material should reflect this atmospheric trend if either (i) DIC governed by atmospheric CO_2 signature or (ii) a high percentage of C from metabolized fresh primary biomass is incorporated during shell aragonite precipitation. While the overall trend in the shells was -0.0039‰ yr^{-1}, the global atmospheric trend was much stronger with about -0.0094‰ yr^{-1} between 1990 and 2000 and -0.0295‰ yr^{-1} on average after 1960 (Fig. 6). Even if we consider that the large scatter in shell data due to physiologic influences will decrease the slope of the regression for the shell, the pronounced trend in air signature after 1960 was not reflected in the mussel shells. We can exclude that temperature effects have disguised the atmospheric trend. The equilibrium ^{13}C fractionation during aragonite precipitation relative to CO_2 was determined by Romanek et al. (1992) $\varepsilon_{\text{aragonite-CO2}} = 13.88 - 0.13\,(t°C)$. From this temperature-fractionation relationship an increase in water temperature by 10.6°C would be necessary to compensate the atmospheric change in carbon signature of 0.245‰ over 50 yr. Such an increase in water temperature is highly unlikely and can be excluded when considering air temperature trends from the region (Fig. 2). Hence, the independence of shell signal from atmospheric trends can only be explained by the incorporation of old (before 1960 or even preindustrial) or mixed organic carbon of different age into the shell.

Unionid bivalves are semi-infaunal filter-feeders and their primary food is believed to be fine particulate organic matter suspended in river water (Dettman et al., 1999). However, the

Table 1. Parameters of spherical models fitted to the experimental semivariograms of the outer and inner layers.

Parameter	Outer	Inner	All	Unit
Nugget effect	0.32	0.15	0.25	‰²
Sill	0.67	0.55	0.65	‰²
Range	25	15	21	years
RMSE[a]	0.035	0.063	0.035	‰²

[a] RMSE = root mean squared error between the semivariogram model and the experimental semivariogram.

Table 2. Signatures of potential food sources.[a]

Potential source	C content (%)	C/N	$\delta^{15}N$ (‰)	$\delta^{13}C$ (‰)
Decomposing alder leaves	42.1	24.4	−2.50	−28.03
Roots	41.3	28.5	0.60	−28.37
Coarse detritus	25.7	23.6	−0.68	−28.02
Fine detritus	10.6	13.4	−0.76	−28.23
Fine suspended particulates >30 μm	22.0	12.9	5.00	−26.96

[a] Concentration of fine suspended particulates in brook water is ca. 50 μg L^{-1}.

food source of freshwater pearl mussels is not known in detail and is still subject to speculation. The internal productivity of this stream is low due to the low nutrient level and shading by trees. The main food source therefore probably originates from the terrestrial surroundings. Isotope analysis of possible food sources showed a more or less uniform $\delta^{13}C$ around −28.2‰ with the exception of fine suspended particulates, which are only −27.0‰ (Table 2). Differences in signatures are even larger for $\delta^{15}N$, which ranged from zero to −2.5‰ for all materials except for the fine suspended particulates, which were 5.0‰, and which were two trophic levels above other sources if we assume a trophic shift of 3‰ per level (De Niro and Epstein, 1981; Ponsard and Averbuch, 1999).

For molluscs, the trophic level shift is only 1 to 2‰, presumably because they excrete ammonium instead of urea or uric acid (Vanderklift and Ponsard, 2003). This is in agreement with the comparison between visceral mass, which consisted mainly of partly digested food, and the remaining body mass (Table 3). The trophic level shift for C in general is small, around 1‰ (De Niro and Epstein, 1981), which is also reflected by the difference between visceral mass and remaining body mass. Hence, the most likely food source should have had a $\delta^{15}N$ of around 5‰ and a $\delta^{13}C$ around −27‰. Both conditions were only met by the fine suspended particulates, which most likely contribute the main share to the mussel diet. The high ^{15}N value in this material in comparison with primary plant biomass indicates that it has passed considerable degradation and recycling. Hence, it is likely old and composite material of different age. In such material the atmospheric signal should be weaker than in air or primary biomass.

In principle, the carbon may stem from mussel respiration of organic material (food) or from riverine DIC, which is influenced by atmospheric CO_2 and environmental respiration (community respiration and input of runoff, soil water and groundwater carrying DIC derived from old plant matter). Assuming an air $\delta^{13}C$ signature of −7.8‰, and a fractionation of aragonite formation relative to CO_2 according to Romanek et al. (1992), then at a water temperature of 10°C a $\delta^{13}C$ value of +4.2‰ would be expected for aragonite formed at isotopic equilibrium. This differs considerably from the values measured in the shells. Analogously, we can assume a food signature of −27‰. A calculation of food consumption and respiration of the mussels indicates that for shell formation (on average: 0.09 g yr^{-1} $mussel^{-1}$), less than 10% of the respired CO_2 is needed, which allows discrimination to take place during aragonite formation. If this metabolically derived carbon is converted to aragonite, applying the fractionation factor as mentioned above, at 10°C a $\delta^{13}C$ value of −15.2‰ would be expected.

Table 3. Average signatures of mussel tissues.

Parameter	n	$\delta^{15}N$	SE	$\delta^{13}C$	SE
Overall average	31	6.90	0.26	−26.10	0.16
Shell organic matter	16	6.81	0.41	−26.15	0.31
Body without visceral mass	13	7.27	0.95	−26.02	0.47
Visceral mass	2	5.80	1.84	−26.29	1.66

The shell signature and its variation can thus be explained by a varying contribution of air and respiratory C (mussel respiration or community respiration contributing to DIC) to the aragonite formation, with respiratory C contributing the largest share. The high contribution of respiratory CO_2, the variation among mussels and the weak to missing correlation with water properties over years are concordant with our perception that the variation in shell signature is of metabolic origin. A calculation of dissolved gasses based on Henry's law and water properties (temperature, pH, ionic strength) indicates that about reasonable 10% of the oxygen dissolved in the inhaled water has to be converted to CO_2 to balance the dissolved carbon species (CO_2, HCO_3^-, CO_3^{2-}) and thus can create a 50% metabolic signal in aragonite precipitated from the exhaled water. The lack of knowledge about the physiology and metabolic activity of freshwater pearl mussels, however, allows no interpretation of the correspondence between differences in signatures and physiologic states. Investigations of the signature of recently precipitated shell material may allow to identify organisms in different physiologic state and thus to gain better insight into this organism.

3.4. Mussels Show Individual Signals

Both shell valves from Z3 showed a clear similarity (Fig. 7), indicating the reliability of the analyses. The variance between the outer layers of the two valves (0.44‰^{2}) was close to the nugget effect (0.36‰^{2}). The nugget effect is estimated from the variation between adjacent layers of one valve and therefore independent from the correspondence of absolute years, to which the layers of both valves are assigned. The similarity of both values indicated that only little additional error results from assigning the layers to years. The same conclusion can be drawn from the comparison between the prismatic and nacreous layers of individual mussels (Fig. 8), which exhibited similar patterns, although an offset between prismatic and nacreous layers extending over several years was often observed.

While the patterns of the prismatic and nacreous layers of one individual were similar, those of different individuals did not match, even assuming errors in assignment to the time axis of single growth increments. This is a strong indication that physiologic processes exert predominant influence on shell $\delta^{13}C$ patterns. This interpretation is supported by the strong negative correlation of body tissue signatures with signatures of the youngest shell layers (Fig. 4). Additionally, total protein mass in the soft tissue negatively correlated with body signature (r^2 = 0.76). The body mass varied by a factor of 3

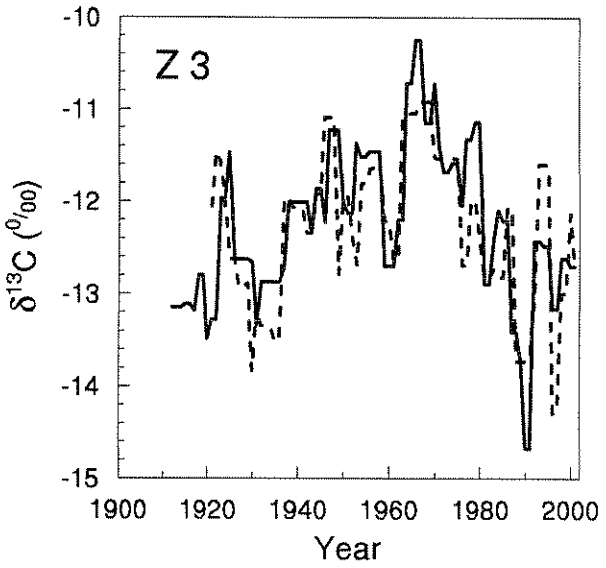

Fig. 7. Variation of $\delta^{13}C$ between successive prismatic layers of both valves from mussel Z3.

(containing 0.5–1.5 g dry matter of protein) despite the similar and high age of the mussels. The studied specimens covered the whole mass range observed in freshwater pearl mussels at this site (Schreckenbach, 1995). This clearly indicates that they differed in metabolic state. The strong correlation with signature suggests that low-weight mussels (e.g., due to starvation or high metabolic activity and production of glochidia) preferentially respire the isotopically lighter amino acids, resulting in a lower body mass, which is isotopically enriched in ^{13}C. The increased use of isotopically lighter lipids (average difference to protein in our samples: −2.8‰) falls short, as their total amount is too low (<1% of body dry matter in all cases) to explain the observed pattern. Indeed, individual differences in the gross energy and soft tissue composition of female mussels from the same river were previously described (Schreckenbach, 1995). This study also revealed losses of 50% in gross energy and strong reduction of dry mass for *Anodonta anatina* mussels kept in tanks for 6 months without feeding. The strong correlation between body protein $\delta^{13}C$ signature and total body signature of mussels can be explained by the fact that 60%–70% of the total dry mass of mussel tissue is made up by the raw protein fraction (Schreckenbach, 1995).

Indeed, environmental parameters averaged over the growth period explained very little to none of the variation in annual signature with r^2 being 0.047, 0.001, 0.0006 and 0.0005 for temperature, pH, conductivity and summer rainfall, respectively. Despite this low predictive ability, the correlation to temperature was highly significant due to the large number of samples (n = 150 in each case). The slope was positive although fractionation decreases with temperature (Romanek et al., 1992). This indicates that the $\delta^{13}C$ of carbon source increased during the warmer months of the year, e.g., by increasing contribution of metabolic vs. water derived CO_2. From the geostatistical analysis it followed that the periods of different metabolic activity extended up to 25 yr. Factors like individual age, gender-associated differences, fecundity and filtering activity are related to metabolic activity and may result in varying body composition and shell carbon signatures between individuals exposed to the same environment. Dettman et al. (1999) found a 4 to 5‰ increase in shell $\delta^{13}C$ in North American freshwater mussels in early August when changes in temperature and $\delta^{13}C$ of DIC were minimal. They state that this change may be associated with the hatching and brooding of young in the marsupia. Metabolic differences between male and female mussels together with the highly variable fecundity among female pearl mussels (Bauer, 1998) could also explain the differences between the individuals investigated in this study. With some annual differences, *M. margaritifera* broods from July to September in the population investigated, which coincides with the period of maximum shell growth. Hence, annual growth increments might be expected to reflect such gender- or fecundity-linked physiologic differences. Individual metabolic activity of pearl mussels may also be linked with genetic factors. Such investigations require high resolution genetic markers, such as microsatellites, which were recently established for the pearl mussel (Geist et al., 2003). For the marine mussel *Mytilus trossulus* Klein et al. (1996) showed that shell $\delta^{13}C$ was influenced by the rate of mantle metabolic activity and Wefer and Berger (1991) reviewed several studies and stated that $\delta^{13}C$ was recording metabolic activity and reproductive activity, which agrees with our results for the freshwater pearl mussel.

Differing filtering activities and food uptake could also be possible explanations for differences between individuals. Borchardt (1985) found an exponential increase of carbon incorporation efficiency and approximately linear increasing net corporation efficiency with decreasing food rations in the blue mussel *Mytilus edulis*.

Kinetic isotope fractionation effects during carbonate precipitation appear to be more likely in aragonites than in calcites and are expressed when calcification occurs within thin, alkaline, Ca^{2+}-rich solutions separated from adjacent cells by CO_2-permeable membranes (McConnaughey et al., 1997). These effects could, in theory, cause considerable variation in shell $\delta^{13}C$; however, this would only occur during rapid carbonate precipitation and thus could only be expected during rapid skeletogenesis (McConnaughey, 1989). Therefore, kinetic isotope effects are highly unlikely to play a role in shell formation for these slowly growing pearl mussels.

Theoretically, the differences between individual signals could also be explained by the exposure of individuals to different environmental conditions, resulting from (i) mussel migration or translocation from other sites or (ii) the existence of different microhabitats within the brook. As the investigated population has been well monitored, migration or translocation events can be excluded for at least 15 yr and especially for the last 4 yr before sampling. Different microhabitats, e.g., different pH linked with algae or submerse vegetation, cannot be fully excluded for the past, but flow turbulences result in a well-mixed water body. Even assuming the occurrence of different sediment microhabitats in this stream with differing CO_2/O_2 ratios, the mussels would still all be exposed to the same water since adult pearl mussels do not bury themselves into the sediments at this site but inhale and infiltrate water from the free-flowing, well-mixed and well-aerated water body. Homogenous water chemical conditions around the mussel

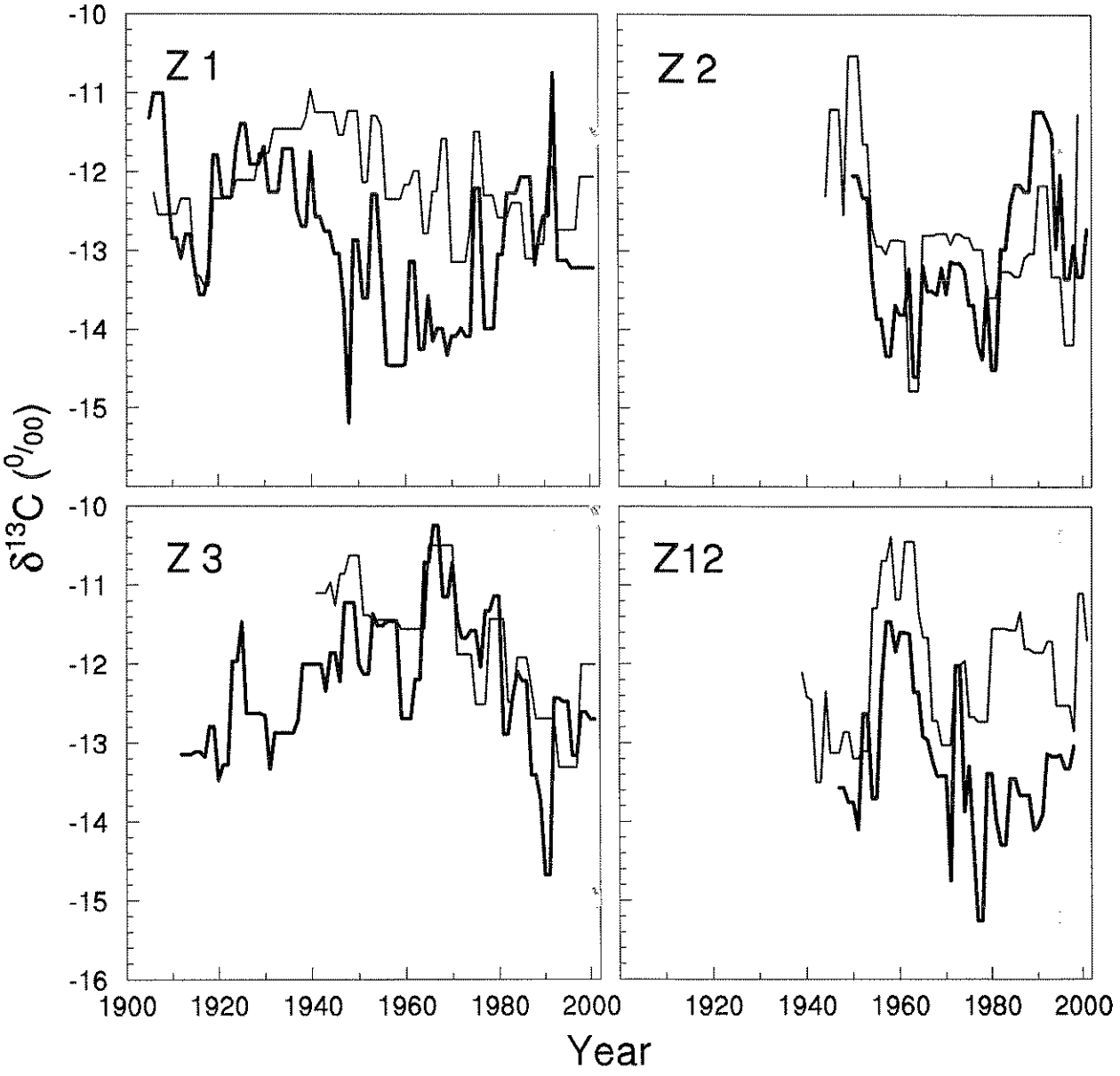

Fig. 8. Comparison of $\delta^{13}C$ patterns from all four mussels; thick lines are outer prismatic layers, and thin lines are inner nacreous layers.

bank were also supported by spatially resolved (<1 m) measurements of temperature, conductivity and pH, which never showed significant differences in the flowing water body during measurements over several years.

4. CONCLUSIONS

The shells of freshwater pearl mussels provide a long-term stable carbon isotope archive, extending up to 100 yr for Central European populations. By heating at 550°C this archive can be easily separated into individual layers, which can then be assigned to single years. This separation is easier for the thick outer prismatic layers than for the thin inner nacreous layers. The outer layers are preferable for sampling in this respect, although some information from early growth stages may be lost by erosion of the oldest layers.

Following the findings of previous authors, shell carbonate is derived from ambient DIC and metabolic derived CO_2. The shells exhibit distinct patterns, which are for each individual similar for both valves and also for the inner nacreous and the outer prismatic layers. Different individuals, which lived within 5 m of each other, and have been exposed to identical environmental conditions, have very different $\delta^{13}C$ patterns in their shells and soft tissues. The negative correlation of soft tissue protein mass with body signature suggests the preferential consumption of isotopically lighter amino acids in periods of starvation or increased metabolic activity, in turn resulting in a

totally lighter but isotopically enriched body. The incorporation of the respired carbon in the aragonite results in a negative correlation between $\delta^{13}C$ signatures of the soft tissues with the youngest shell layers. Additionally, almost no influence of atmospheric CO_2 signature, pH and water temperature on $\delta^{13}C$ patterns was detectable. Consequently, the observed distinct signature patterns of different mussels can not be explained by environmental variables, but metabolic processes must exert predominant influence on shell signatures. Individual signal trends extend up to 25 yr and can cover one-fourth of the life span of the mussel.

Shell aragonite carbon mainly originated from respiration. The lack of an atmospheric trend in the $\delta^{13}C$ of the shell carbonates suggests that the respired carbon source consists of old recycled carbon. This is also in agreement with the $\delta^{15}N$ signatures of the body tissue, which showed a high trophic level. Both, the $\delta^{13}C$ and the $\delta^{15}N$ signatures, indicated that fine suspended particulates (>30 μm) are the most likely food source.

Our results indicate that $\delta^{13}C$ signatures in freshwater mussel shells can strongly be influenced by individual metabolic signals, which prevent these time archives from being used for reconstruction of environmental parameters. This phenomenon should also be taken into account when investigating other mussel species.

Acknowledgments—This study was originally initiated by a student project within the course "Stable isotopes in ecology and plant physiology." We thank K. Schullehner for technical assistance, H. Schnyder and R. Schäufele for stimulating discussions. We are extremely grateful to D. L. Dettman, Arizona, for carrying out comparative measurements of shell $\delta^{13}C$, to H. Stanjek, Aachen, for his help with XRD analyses and to E. Späth and St. Schmidt from the Water Authority Hof for providing additional water chemical data. Detailed comments from T. McConnaughey, D. L. Dettman, and a third, anonymous reviewer were highly appreciated and helped improve an earlier version of the manuscript. J. Geist was supported in this research by "Bayerischer Naturschutzfonds" and "Landesfischereiverband Bayern." A. Boom acknowledges the financial support provided through the European Community's Human Potential Program under contract HPRN-CT-1999-00059, NETCARB.

Associate editor: J. Brandes

REFERENCES

Auerswald K. (1990) Einfluß von Boden-pH und Bodenwasserhaushalt auf die Gewässerversauerung im ostbayerischen Grundgebirge. *Laufener Seminarbeiträge* **4/90**, 23–29.

Bauer G. (1992) Variation in the life-span and size of the fresh-water pearl mussel. *J. Anim. Ecol.* **61**, 425–436.

Bauer G. (1998) Allocation policy of female freshwater pearl mussels. *Oecologia* **117**, 90–94.

Borchardt T. (1985) Relationships between carbon and cadmium uptake in *Mytilus edulis*. *Mar. Biol.* **85**, 233–244.

Carell B., Forberg S., Grundelius E., Henrikson L., Johnels A., Lindh U., Mutvei H., Olsson M., Svardstrom K., and Westermark T. (1987) Can mussel shells reveal environmental history? *Ambio* **16**, 2–10.

Craig H. (1953) The geochemistry of the stable carbon isotopes. *Geochim. Cosmochim. Acta* **3**, 53–65.

De Niro M. J. and Epstein S. (1981) Influence of diet on the distribution of nitrogen isotopes in animals. *Geochim. Cosmochim. Acta* **45**, 341–351.

Dettman D. L. and Lohmann K. C. (1993) Seasonal changes in paleogene surface water $\delta^{18}O$: Fresh-water bivalves of western North America. In *Climate Change in Continental Isotopic Records* Vol. 78 (eds. P. K. Swart et al.), pp. 153–163. AGU.

Dettman D. L., Reische A. K., and Lohmann K. C. (1999) Controls on the stable isotope composition of seasonal growth bands in aragonitic fresh-water bivalves (Unionidae). *Geochim. Cosmochim. Acta* **63**, 1049–1057.

Donner J. and Nord A. G. (1986) Carbon and oxygen stable isotope values in shells of *Mytilus edulis* and *Modiolus modiolus* from Holocene raised beaches at the outer coast of the Varanger peninsula, North Norway. *Palaeogeogr. Palaeoclimatol. Palaeoecol.* **56**, 35–50.

Epstein S., Buchsbaum R., Lowenstam H. A., and Urey H. C. (1953) Revised carbonate-water isotopic temperature scale. *Geolog. Soc. Amer. Bull.* **64**, 1315–1325.

Friedli H., Lötscher H., Oeschger H., Siegenthaler U., and Staffer B. (1986) Ice core record of the $^{13}C/^{12}C$ ratio of atmospheric CO_2 in the past two centuries. *Nature* **324**, 237–238.

Fritz P. and Poplawski S. (1974) ^{18}O and ^{13}C in shells of freshwater molluscs and their environments. *Earth. Planet. Sci. Lett.* **24**, 91–98.

Fry B. and Allen Y. C. (2003) Stable isotopes in zebra mussels as bioindicators of river-watershed linkages. *River Res. Appl.* **19**, 683–696.

Geist J., Rottmann O., Schröder W., and Kühn R. (2003) Development of microsatellite markers for the endangered freshwater pearl mussel Margaritifera margaritifera L. (Bivalvia: Unionoidea). *Mol. Ecol. Notes* **3**, 444–446.

Harris D., Horwath W. R., and van Kessel C. (2001) Acid fumigation of soils to remove carbonates prior to total organic carbon or carbon-13 isotopic analysis. *Soil Sci. Soc. Am. J.* **65**, 1853–1856.

Hastie L. C., Young M. R., and Boon P. J. (2000) Growth characteristics of freshwater pearl mussels, *Margaritifera margaritifera* (L.). *Freshwater Biol.* **43**, 243–256.

Kaandorp R. J. G., Vonhof H. B., Del Busto C., Wesselingh F. P., Ganssen G. M., Marmól A. E., Pittman L. R., and van Hinte J. E. (2003) Seasonal stable isotope variations of the modern Amazonian freshwater bivalve *Anodonitites trapesialis*. *Paleogeogr. Paleoclimatol. Palaeoecol.* **194**, 339–354.

Keeling C. D., Whorf T. P., Wahlen M., and van der Plicht J. (1995) Interannual extremes in the rate of rise of atmospheric carbon-dioxide since 1980. *Nature* **375**, 666–670.

Keith M. L., Anderson G. M., and Eichler R. (1964) Carbon and oxygen isotopic composition of mollusk shells from marine and fresh-water environments. *Geochim. Cosmochim. Acta* **28**, 1757–1786.

Klein R. T., Lohmann K. C., and Thayer C. W. (1996) Sr/Ca and $^{13}C/^{12}C$ ratios in skeletal calcite of *Mytilus trossulus*: Covariation with metabolic rate, salinity and carbon isotopic composition of seawater. *Geochim. Cosmochim. Acta* **60**, 4207–4221.

Lindh U., Mutvei H., Sunde T., and Westermark T. (1988) Environmental history told by mussel shells. *Nucl. Instrum. Methods Phys. Res. Sect. B* **30**, 388–392.

McConnaughey T. A. (1989) ^{13}C and ^{18}O isotopic disequilibrium in biological carbonates: I. Patterns. *Geochim. Cosmochim. Acta* **53**, 151–162.

McConnaughey T. A. (2003) Sub-equilibrium oxygen-18 and carbon-13 levels in biological carbonates: Carbonate and kinetic models. *Coral Reefs* **22**, 316–327.

McConnaughey T. A., Burdett J., Whelan J. F., and Paull C. K. (1997) Carbon isotopes in biological carbonates: Respiration and photosynthesis. *Geochim. Cosmochim. Acta* **61**, 611–622.

Mook W. G. (1971) Paleotemperatures and chlorinities from stable carbon and oxygen isotopes in shell carbonate. *Palaeogeogr. Palaeoclim. Palaeoecol.* **9**, 245–263.

Mutvei H. and Westermark T. (2001) How environmental information can be obtained from Naiad shells. In *Ecology and Evolution of the freshwater mussels Unionoida. Ecological Studies*, Vol. 145 (eds. G. Bauer and K. Wächtler), Springer, Heidelberg, pp. 367–379.

Nielsen D. R. and Wendroth O. (2003) *Spatial and Temporal Statistics.* Reiskirchen, Catena Verlag.

Nyström J., Lindh U., Dunca E., and Mutvei H. (1995) A study of *Margaritifera margaritifera* shells from the river Paulistromsan, S. Sweden. *Nucl. Instrum. Methods Phys. Res. Sect. B* **104**, 612–618.

Piasentier E., Valusso R., Camin F., and Versini G. (2003) Stable isotope ratio analysis for authentication of lamb meat. *Meat Sci.* **64,** 239–247.

Ponsard S. and Averbuch P. (1999) Should growing and adult animals fed on the same diet show different $\delta^{15}N$ values? *Rapid Commun. Mass Spectrom.* **13,** 1305–1310.

Romanek C. S., Grossman E. L., and Morse J. W. (1992) Carbon isotopic fractionation in synthetic aragonite and calcite—Effects of temperature and precipitation rate. *Geochim. Cosmochim. Acta* **56,** 419–430.

Rossmann A. (2001) Determination of stable isotope ratios in food analysis. *Food Rev. Int.* **17,** 347–381.

Schreckenbach K. (1995) Untersuchungen zum Ernährungszustand von Flußperl- und Teichmuscheln (*Margaritifera margaritifera* und *Anodonta anatina*). *Lindberger Hefte* **5,** 84–97.

Siegele R., Orlic I., Cohen D. D., Markich S. J., and Jeffree R. A. (2001) Manganese profiles in freshwater mussel shells. *Nucl. Instrum. Methods Phys. Res. Sect. B* **181,** 593–597.

Tanaka N., Monaghan M. C., and Rye D. M. (1986) Contribution of metabolic carbon to mollusc and barnacle shell carbonate. *Nature* **320,** 520–523.

Tripati A., Zachos J., Marincovich L., and Bice K. (2001) Late Paleocene Arctic coastal climate inferred from molluscan stable and radiogenic isotope ratios. *Palaeogeogr. Palaeoclimatol. Palaeoecol.* **170,** 101–113.

Vander Putten E., Dehairs F., Keppens E., and Baeyens W. (2000) High resolution distribution of trace elements in the calcite shell layer of modern *Mytilus edulis*: Environmental and biological controls. *Geochim. Cosmochim. Acta* **64,** 997–1011.

Vanderklift M. A. and Ponsard S. (2003) Sources of variation in consumer-diet δN^{15} enrichment: A meta-analysis. *Oecologia* **136,** 169–182.

Veinott G. I. and Cornett R. J. (1998) Carbon isotopic disequilibrium in the shell of the freshwater mussel *Elliptio complanata*. *Appl. Geochem.* **13,** 49–57.

Wefer G. and Berger W. H. (1991) Isotope paleontology: Growth and composition of extant calcareous species. *Mar. Geol.* **100,** 207–248.

Wurster C. M., Patterson W. P., and Cheatham M. M. (1999) Advances in micromilling techniques: A new apparatus for acquiring high-resolution oxygen and carbon stable isotope values and major/minor elemental ratios from accretionary carbonate. *Comput. Geosci.* **25,** 1159–1166.

Stable carbon isotopes in freshwater mussel shells: Environmental record or marker for metabolic activity?

Karl Auerswald[1)], Jürgen Geist[1)], Arnoud Boom[1)]

[1)] *Wissenschaftszentrum Weihenstephan, TU München, D-85350 Freising*
auerswald@wzw.tum.de

The ^{18}O signature of shells is frequently used as environmental proxy, whereas the control of ^{13}C signature is poorly understood. Aragonitic shell material from an extant, long-living freshwater bivalve, the freshwater pearl mussel *Margaritifera margaritifera* L., provides a long-term (80 yr) ^{13}C archive, which might provide insight into environmental or metabolic changes.

The archive could easily be separated into individual layers and chronologically assigned to years after heating at 550°C. This is superior to previously used methods. The separation was easier for the thick outer prismatic layers than for the thin inner nacreous layers. Outer layers are preferable in this respect although some information may be lost by corrosion of the oldest layers.

The ^{13}C signature of the layers was mainly created by metabolic processes and not by environmental signals resulting in similar patterns of inner and outer layers and on both valves within one mussel, but differing patterns between mussels in close neighborhood. The individual pattern extended up to 25 years and cover thus one fourth of the life span of the mussel.

The carbon in shell aragonite mainly (>80%) originated from respiration, with filter material (<30 µm) being the main food source of the mussel. Nitrogen isotope signature of the filter material showed that it is old, recycled material, which explains why the global trend in atmospheric CO_2 signature was only weakly reflected by the shell aragonite. Very low (<-14 ‰) ä^{13}C values indicated Rayleigh fractination with only little respiration and a large fraction of the respiratory C needed for shell formation. This could indicate starvation and explain the low fertility and high mortality of freshwater pearl mussels at the experimental site although the lowest values did not coincide with the last year of living.